Electronic-Structures Calculations of Calcium-Intercalated Bilayer Graphene: A First-Principle Study

Sri Hidayati[1,2], Iman Santoso[1], Sefty Yunitasari[1], and Sholihun Sholihun[1*]

[1]*Computational Physics Research Group, Department of Physics, Faculty of Mathematics and Natural Sciences, Universitas Gadjah Mada, Sekip Utara BLS 21, Yogyakarta 55281, Indonesia*

[2]*Department of Physics, Faculty of Science and Technology, Universitas Islam Negeri Sunan Kalijaga, Jl. Laksda Adisucipto, Yogyakarta 55281, Indonesia*

* ***Corresponding author:***

email: sholihun@ugm.ac.id

Received: June 22, 2022
Accepted: September 15, 2022

DOI: 10.22146/ijc.75647

Abstract: *In this study, electronic structure calculations of Ca-intercalated bilayer graphene are conducted using the density functional theory (DFT). We modeled two configurations by positioning calcium in the middle of the bilayer (M-site) and on top of the bilayer surface (T-site). Our results show that the Dirac point is shifted below the fermi level. The approximated critical temperature is 7.9 K. We then calculated the electron transfer and formation energy for each system. We found that, for the M-site, the electron transfer increased as the Ca concentration increased, while the reverse occurred for T-site. The calculated formation energies were negative, meaning that all configurations were spontaneously created. In other words, the involved reactions were exothermic.*

Keywords: *Ca-intercalated bilayer graphene; formation energy; electronic structure*

■ INTRODUCTION

Carbon has several allotropes, such as graphite, diamond, and carbon nanotubes [1]. Among these, graphite, consisting of multilayer carbon atoms connected by Van der Waals's bonds, is the most stable material at room temperature. Graphene, monolayer graphite successfully fabricated [2], has drawn much interest because of its distinct electrical structure and mechanical and thermal characteristics. [3-6]. Such characteristics allow graphene to have potential applications. For example, they are used as hydrogen storage materials and chemical sensors [7-9].

The atomic doping of silicon, boron, nitrogen, phosphorus, sulfur, aluminum and gallium [10-13] in graphene changes its electronic structure [10,14]; for example, it can result in a finite bandgap opening at the K-point, causing graphene to behave as a semiconductor. Recently, theoretical studies showed that the superconductivity effect was investigated in Ca- and Li-doped monolayers and bilayer graphene [7,15-17]. Therefore, an investigation of atomic-doped graphene, particularly Ca-doped bilayer graphene, is necessary.

In the present study, we performed DFT calculations to analyze the effect of Ca-intercalated bilayer graphene on electronic structures and to determine the trade-off doping concentration. The doping concentrations were varied up to 6.25%. We involved a 64 atomic-sites supercell in calculating formation energies, the density of states (DOS), and band structures.

■ COMPUTATIONAL METHODS

We calculated the structural and electronic structures of the Ca-doped bilayer. We used the code PHASE, a quantum-based simulation with plane wave basis sets [18-25]. The generalized gradient approximation (GGA) based on the Perdew-Burke-Ernzerhof (PBE) functional was chosen as the exchange correlation. We relaxed atoms so that the atomic forces are less than 5.0×10^{-3} eV/Å. We set a 15 Å vacuum parameter to avoid interlayer interactions.

The bilayer graphene was simulated in a 64 atomic-sites supercell, obtained by expanding a $4 \times 4 \times 1$ for the atomic-sites unit cell. We then doped the bilayer graphene with Ca in two positions: in the middle between

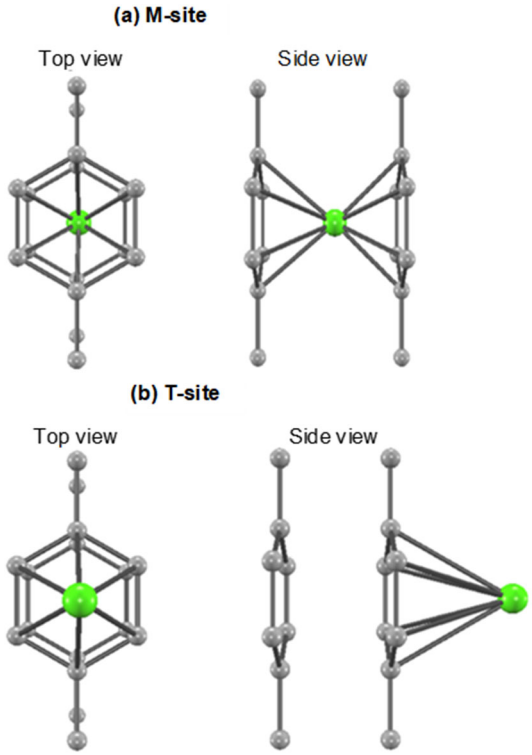

Fig 1. The geometry of the (a) M-site and (b) T-site Ca-intercalated bilayer graphene

two layers (M-site, Fig. 1(a)) and on the top of the bilayer (T-site, Fig. 1(b)). The atomic positions of Ca are set near the middle of the hexagonal lattice (hollow site) to maintain the symmetry of the graphene lattice. We varied the Ca concentration and calculated the DOS and band structures.

The formation energies were calculated as follows:

$$E_f = E_T - E_g - m\mu_i \quad (1)$$

where E_f is the formation energy, E_T is the total energy of the flawed system, E_g is the total energy of the pristine, m is the number of doped atoms, and μ_i is the chemical potential of calcium.

The charge transfer from Ca to graphene was calculated using the following equation Ref. [3]

$$q(e) = \frac{\left(E_D - E_{fermi}\right)^2}{\pi\left(\hbar\right)^2} \quad (2)$$

where q(e), E_D, and E_{fermi} are the charge transfer, energy at the Dirac point, and energy at the Fermi level, respectively.

■ RESULTS AND DISCUSSION

Optimized Geometry

First, we optimized the unit cell and found that the optimized lattice constant was 2.48 Å, close to an experimental result of 2.46 Å [26]. We then doped Ca on the bilayer graphene. Since graphene has a high-symmetry hexagonal structure, the high-symmetry position of the hollow site has been found as the most stable position [28]. We placed Ca on the hollow site of the middle (M-site, Fig. 1(a)) and the top surface of the bilayer graphene (T-site, Fig. 1(b)). The defect geometry in the M-site is symmetrical under a C_6 symmetry element (rotation $\frac{2\pi}{6}$) and horizontal mirror σ_h; thus, the M-site Ca-doped bilayer graphene belongs to a C_{6v} symmetry. Meanwhile, the T-site one belongs to a C_{6v} because of the absence of σ_h.

We used Ca concentrations of 1.5% (Fig. 2(a) and 2(d)), 3.12% (Fig. 2(b) and 2(e)), and 6.25% (Fig. 2(c) and 2 (f)). The optimized structures of each system are given in Fig. 2. We then calculated the structural properties, which are presented in Table 1. In both the M- and T-sites, Ca was strongly bounded via covalent bonds, which agrees with the result in Ref. [27], which also mentions that Ca was strongly bounded by graphene. The calculated distances between the two closest carbon atoms (C–C) in the pristine graphene were found to be 1.43 Å, which agrees with the experimental result (1.42 Å) [3]. Moreover, the distances of C–C in the flawed system were between 1.42 and 1.43 Å, while the calculated distances C–Ca were between 2.70 and 2.80 Å (Table 1). The distance between layers (c_1) in the flawed system was somewhat larger (ranging from 3.80 and 4.66 Å) than that in the pristine one (3.66 Å).

The formation energies calculated using Eq. (1) are presented in Table 1. The T-site was energetically more favorable than the M-site, as shown by the smaller absolute value of the formation energies; that is, the energy of the T-site with one adatom was 0.52 eV less than that of the M-site. However, the configurations of both the M- and T-sites were spontaneously created since

Table 1. Structural properties: Distance between neighboring carbon atoms (C–C), distances between C and Ca (C–Ca), distances between layer c (Å), formation energy E_f, Energy at the Dirac-point E_D, and electron transfer q(e)

Concentration (%)	Position	D_{C-C} (Å)	D_{C-Ca} (Å)	C_l (Å	E_f (eV)	E_D (Å)	q (e)
0.00	–	1.432	–	3.66	–	–	–
1.56	M	1.428	2.714	4.53	−1.47	0.97	0.03
3.12	M	1.430	2.755	4.66	−2.07	1.1	0.04
6.25	M	1.427	2.703	4.50	−3.67	1.37	0.06
1.56	T	1.427	2.674	4.11	−0.10	0.52	0.0087
3.12	T	1.425	2.854	4.05	−0.33	0.47	0.0075
6.25	T	1.419	2.788	3.84	−1.18	0.12	0.0004

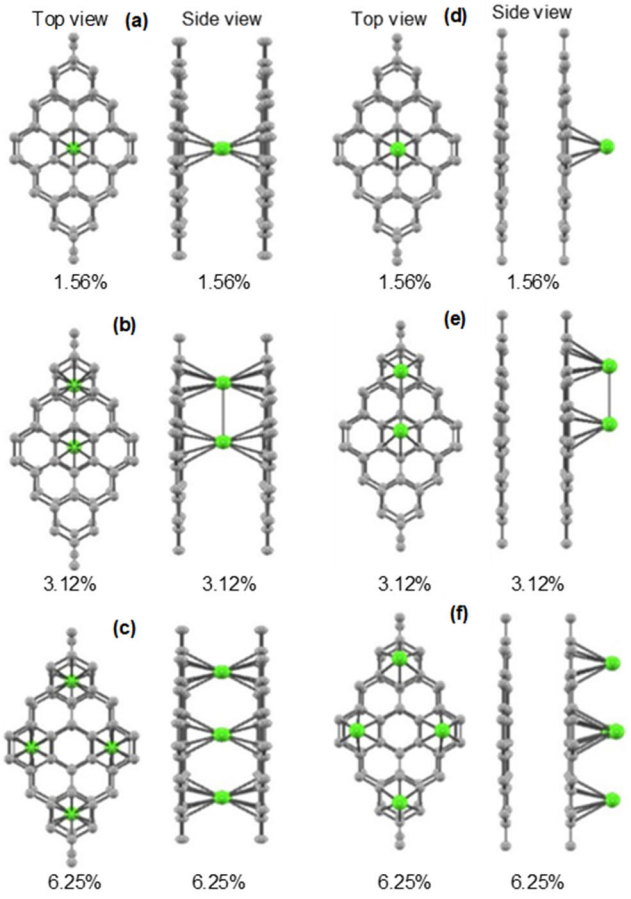

Fig 2. Optimized geometries of Ca-intercalated bilayer graphene: M-site (a) 1.56%, (b) 3.12%, (c) 6.25%, and T-site (d) 1.56%, (e) 3.12%, (f) 6.25%

the formation energy values were negative, corresponding to an exothermic reaction.

Electronic Structures

We calculated the band structures and DOS of both systems. The band structures of the pristine bilayer graphene consisted of two valence bands (π) and two conduction bands (π*) Fig. 3. The Dirac point lies on the K-point, forming a linear dispersion in the Fermi level. Therefore, the pristine bilayer graphene was semimetallic, which is consistent with the results of the previous studies [2,4]. The Fermi level was set to zero for both band structures and DOS in Fig. 3.

The calculated band structures and DOS of Ca-intercalated bilayer graphene with concentrations of 1.56, 3.12, and 6.25% are given in Fig. 4 and Fig. 5 for the M-site and T-site, respectively. As in the pristine, both systems have two valence and conduction bands, crossing each other, producing a linear dispersion near the Dirac point. However, in the case of M-site, these two bands coincide in Dirac-point.

If the Dirac point in the pristine lies at the Fermi level, that in the Ca-doped bilayer, graphene would be shifted down from the Fermi level. The shifted Dirac point is due to the electron transfer from Ca to graphene, causing Ca behave as n-type. The doping concentration also influences the number of electron transfers. In the case of the M-site with the highest doping concentration (6.25%), the electron transfer is about 0.06 e, while in the case of the T-site, it is about 0.0004 e.

The value of Dirac-point shift both the M-site has DOS peaks of 74, 88, and 83 states/eV (Fig. 4) while the T-site has DOS peaks of 78, 8, and 75 v states/eV for the concentration of 1.56, 3.12, and 6.25% (Fig. 5), respectively. Overall, M-site and T-site have similar trends of DOS, e.g., the magnitude of states of each system decreases compared to DOS in the pristine. For instance, at 8.2 eV for concentration 1.56%, the DOS decreases from 92 states/eV (in pristine) to 47 states/eV (in the M-site) and to 42 states/eV (in the T-site).

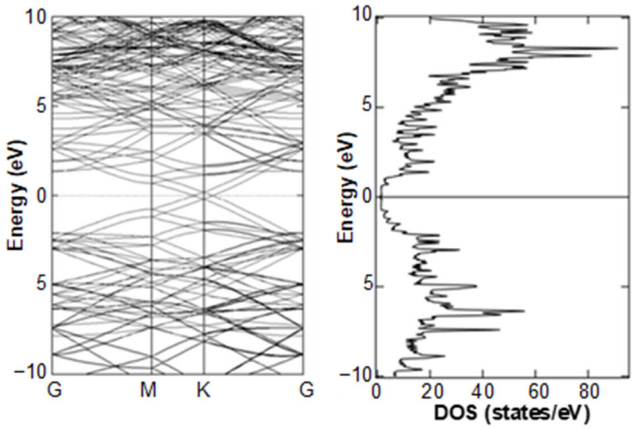

Fig 3. Band structure and density of states for pristine bilayer graphene

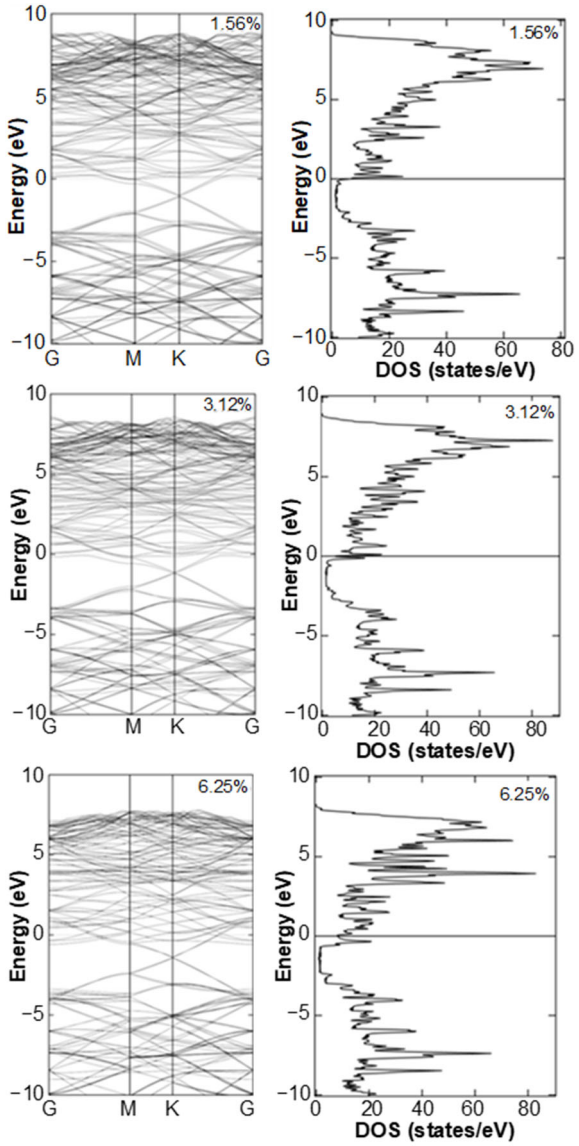

Fig 4. Band structure and density of states for M-site

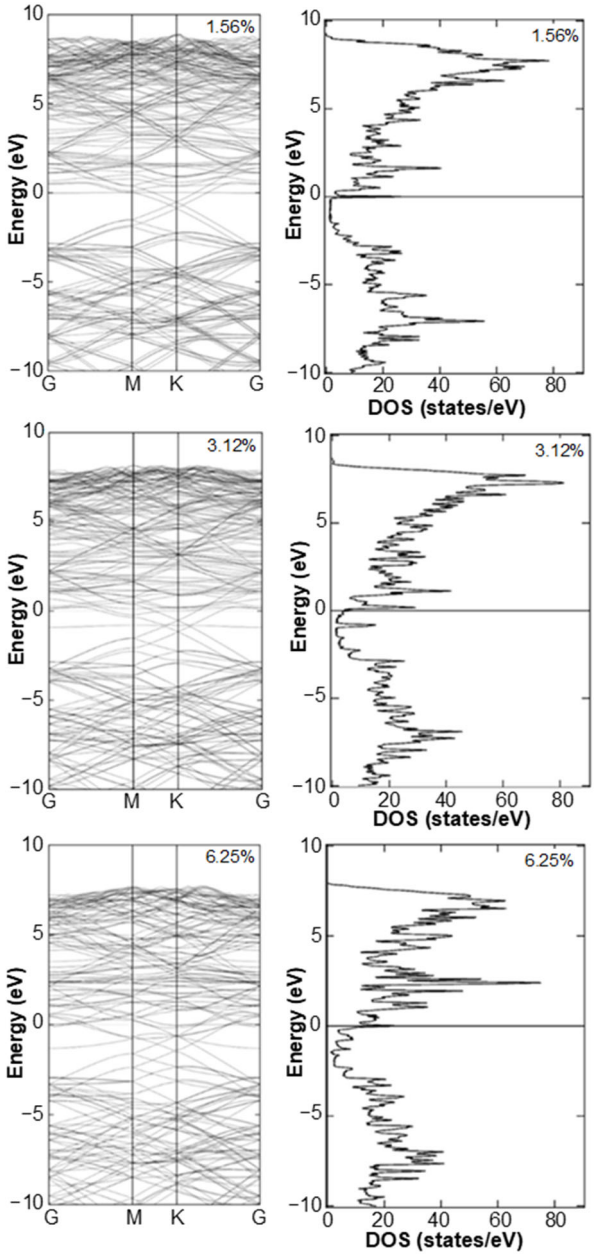

Fig 5. Band structure and density of states for T-site

The Van Hove states are also shifted down to the Fermi level, allowing electrons to occupy these states. The DOS shows this behavior in Fig. 4 and 5. Therefore, the Ca-intercalated bilayer graphene is metallic [15,28]. The shift in Dirac point increased as the Ca concentration increased. However, the concentration of 6.25% on the bilayer graphene affects band structures; for example, some new states appear around the Dirac point.

In addition, a flat band was formed on the T-site at concentrations of 1.56 and 3.12% (Fig. 5). The flat band

also appeared near the Fermi level in the previous studies [29-31]. It was predicted that superconductivity on the flat band area could be achieved at a higher T_c (critical temperature) [29,32]. In this state, electrons are very likely to occupy. In our calculation at a concentration of 6.25%, this flat band tended to disappear; thus, we conclude that the maximum trade-off Ca-doping concentration in bilayer graphene is 6.25%. The critical temperature T_c can be approximated using $k_B T_c = 1.13\theta_D e^{-1/\lambda}$ and $\lambda = \frac{N(0)D^2}{M\omega_{ph}^2}$, where k_B, θ_D, λ, N(0), D, M and ω_{ph}^2 are the Boltzmann constant, Debye temperature (15 K), electron-phonon coupling constant, DOS per spin at the Fermi level, deformation potential, effective atomic mass, and phonon frequency, respectively. For instance, our calculated N(0) for the T-site is 13.11 eV^{-1}. Using a ω_{ph} of 0.16 eV [17], D of 0.66, [33] and λ of ≈ 0.1 N(0), a T_c of approximately 7.5 K was predicted. The calculated T_c is 3.5 K higher than the T_c of the experimental result (4 K) [15]. This difference in Tc is caused by the varied Ca concentrations; for instance, the current work's Ca concentration is 6.25%, whereas that of C_6CaC_6 is 8.33%. However, phonon calculations are necessary for further clarification.

Furthermore, we calculated the charge transfer using Eq. (2). In the case of the M-site, the electron transfer q(e) increased as the concentration increased; however, the reverse happened in the T-site due to the shifted Dirac-point from the Fermi level (E_D). We show in Table 1 that the most significant electron transfer corresponded to the M-site at a concentration of 6.25%.

■ CONCLUSION

We calculated the structural and electronic properties of Ca-intercalated bilayer graphene. From the calculated formation energy, we found that the T-site is energetically more favorable than the M-site. The Ca adatoms affected the band structures; for example, the Dirac point was shifted down from the Fermi level, causing Ca to behave as n-type. From the calculated charge transfer, the most significant charge transfer, 0.06 e, was found in the M-site at a concentration of 6.25%. This result can contribute to the research of graphene-based electronic devices.

■ ACKNOWLEDGMENTS

We thank the Ministry of Education, Culture, Research, and Technology of Indonesia for the research facilities through the "*Penelitian Dasar 2022*" research grant No. 018/E5/PG.02.00.PT/2022; 1710/UN1/DITLIT/Dit.Lit/PT.01.03/2022.

■ REFERENCES

[1] Emery, N., Hérold, C., Marêché, J.F., and Lagrange, P., 2010, Synthesis and superconducting properties of CaC_6, *Sci. Technol. Adv. Mater.*, 9 (4), 044102.

[2] Novoselov, K.S., Geim, A.K., Morosov, S.U., Jiang, D., Zhang, Y., Dubonos, S.V., Grigorieva, I.V., and Firsov, A.A., 2004, Electric field effect in atomically thin carbon films, *Science*, 306 (5696), 666–669.

[3] Castro Neto, A.H., Guinea, F., Peres, N.M.R., Novoselov, K.S., and Geim, A.K., 2009, The electronic properties of graphene, *Rev. Mod. Phys.*, 81 (1), 109–162.

[4] Novoselov, K.S., Jiang, D., Schedin, F., Booth, T.J., Khotkevich, V.V., Morosov, S.V., and Geim, A.K., 2005, Two-dimensional atomic crystals, *Proc. Natl. Acad. Sci. U.S.A.*, 102 (30), 10451–10453.

[5] Lee, C., Wei, X., Kysar, J.W., and Hone, J., 2008, Measurement of the elastic properties and intrinsic strength of monolayer graphene, *Science*, 321 (5887), 385–388.

[6] Geim, A.K., and Novoselov, K.S., 2007, The rise of graphene, *Nat. Mater.*, 6 (3), 183–191.

[7] Taghioskoui, M., 2009, Trends in graphene research, *Mater. Today*, 12 (10), 34–37.

[8] Elias, D.C., Nair, R.R., Mohiuddin, T.M.G., Morosov, S.V., Blake, P., Halsall, M.P., Ferrari, A.C., Boukhvalov, D.W., Katsnelson, M.I., Geim, A.K., and Novoselov, K.S., 2009, Control of graphene's properties by reversible hydrogenation: Evidence for graphene, *Science*, 323 (5914), 610–613.

[9] Schedin, F., Geim, A.K., Morosov, S.V., Hill, E.W., Blake, P., Katsnelson, M.I., and Novoselov, K.S., 2007, Detection of individual gas molecules adsorbed on graphene, *Nat. Mater.*, 6 (9), 652–655.

[10] Rofique, M., Shuai, Y., and Hussain, N., 2018, First-principles study on silicon atom doped monolayer graphene, *Phys. E*, 95, 94–101.

[11] Laref, A., Ahmed, A., Bin-Omran, S., and Luo, S.J., 2015, First-principle analysis of the electronic and optical properties of boron and nitrogen doped carbon mono-layer graphenes, *Carbon*, 81, 179–192.

[12] Shokuhi Rad, A., Zareyee, D., Peyravi, M., and Jahanshahi, M., 2016, Surface study of gallium- and aluminum- doped graphenes upon adsorption of cytosine: DFT calculations, *Appl. Surf. Sci.*, 390, 444–451.

[13] Dennis, P.A., 2016, Mono and dual doped monolayer graphene with aluminum, silicon, phosphorus and sulfur, *Comput. Theor. Chem.*, 1097, 40–47.

[14] Santos, E.J.G., Sánchez-Portal, D., and Ayuela, A., 2010, Magnetism of substitutional Co impurities in graphene: Realization of single π vacancies, *Phys. Rev. B*, 81, 125433.

[15] Ichinokura, S., Sugawara, K., Takayama, A., Takahashi, T., and Hasegawa, S., 2016, Superconducting calcium-intercalated bilayer graphene, *ACS Nano*, 10 (2), 2761–2765.

[16] Chapman, J., Su, Y., Howard, C.A., Kundys, D., Grigorenko, A.N., Guinea, F., Geim, A.K., Grigorieva, I.V., and Nair, R.R., 2016, Superconductivity in Ca-doped graphene laminates, *Sci. Rep.*, 6 (1), 23254.

[17] Proveta, G., Calandra, M., and Mauri, F., 2012, Phonon-mediated superconductivity in graphene by lithium deposition, *Nat. Phys.*, 8 (2), 131–134.

[18] The Center for Research on Innovative Simulation Software (CISS), *PHASE*, http://www.ciss.iis.u-tokyo.ac.jp/dl/index.php, accessed on June 20, 2017.

[19] Umam, K., Sholihun, S., Nurwantoro, P., Absor, M.A.U., Nugraheni, A.D., and Budhi, R.H.S., 2018, Biaxial strain effects on the electronic properties of silicene: The density-functional-theory-based calculations, *J. Phys.: Conf. Ser.*, 1011, 012074.

[20] Amalia, W., Nurwantoro, P., and Sholihun, S., 2019, Density-functional-theory calculations of structural and electronic properties of vacancies in monolayer hexagonal boron nitride (h-BN), *Comput. Condens. Matter*, 18, e00354.

[21] Lin, J., Yamasaki, T., and Saito, M., 2014, Spin polarized positron lifetimes in ferromagnetic metals: First-principles study, *Jpn. J. Appl. Phys.*, 53, 053002.

[22] Nurainun, N.Y., Lin, J., Alam, M.S., Nishida, K., and Saito, M., 2011, First-principles calculations of hydrogen and hydrogen-vacancy pairs in graphene, *Trans. Mater. Res. Soc. Jpn.*, 36 (4), 619–621.

[23] Sholihun, S., Amalia, W., Hastuti, D.P., Nurwantoro, P., Nugraheni, A.D., and Budhi, R.H.S., 2019, Magic vacancy-numbers in h-BN multivacancies: The first-principles study, *Mater. Today Commun.*, 20, 100591.

[24] Hastuti, D.P., Nurwantoro, P., and Sholihun, S., 2019, Stability study of germanene vacancies: The first-principles calculations, *Mater. Today Commun.*, 19, 459–463.

[25] Hidayati, S., 2019, Kajian Komputasi Sumbangan Struktur Elektronik Pada Superkonduktivitas Bilayer Graphene Terdoping Kalsium Menggunakan Density Functional Theory, *Thesis*, Universitas Gadjah Mada, Indonesia.

[26] Delley, B., 1990, An all-electron numerical method for solving the local density functional for polyatomic molecules, *J. Chem. Phys.*, 92, 508–517.

[27] Sun, M., Tang, W., Ren, Q., Wang, S., Yu, J., Du, Y., and Zhang, Y., 2015, First-principles study of the alkali earth metal atoms adsorption on graphene, *Appl. Surf. Sci.*, 356, 668–673.

[28] Mazin, I.I., and Balatsky, A.V., 2010, Superconductivity in Ca-intercalated bilayer graphene, *Philos. Mag. Lett.*, 90 (10), 731–738.

[29] Marchenco, D., Evtushinsky, D.V., Golias, E., Varykhalov, A., Seyller, Th., and Rader, O., 2018, Extremely flat band in bilayer graphene, *Sci. Adv.*, 4, eaau0059.

[30] McChesney, J.L., Bostwick, A., Otha, T., Seyller, T., Horn, K., González, J., and Rotenberg, E., 2010, Extended van Hove singularity and superconducting instability in doped graphene,

Phys. Rev. Lett., 104, 136803.

[31] Kiesel, M.L., Platt, C., Hanke, W., Abanin, D.A., and Thomale, R., 2012, Competing many-body instabilities and unconventional superconductivity in graphene, *Phys. Rev. B*, 86 (2), 020507.

[32] Kopnin, N.B., Heikkilä, T.T., and Volovik, G.E., 2011, High-temperature surface superconductivity in topological flat-band system, *Phys. Rev. B*, 83 (22), 220503.

[33] Thomsen, C., Reich, S., and Ordejón, P., 2002, *Ab initio* determination of the phonon deformation potentials of graphene, *Phys. Rev. B*, 65, 073403.